ISSN 2349-6193
Impact Factor (PIF): 2.243

IJESMR
International Journal OF Engineering Sciences & Management Research

FINITE ELEMENT ANALYSIS OF CHIRAL HONEYCOMB WITH ELLIPTICALLY STRUCTURED CENTRAL NODE

Umamaheswaran Shanmugam *, Subramanyam Burlakanti
* P.G.scholar(CAD/CAM), MLRIT,HYDERABAD, India
Asst.Professor, Dept. of Mech.Engg, MLRIT, HYDERABAD, India

Keywords: Chiral, Morphing Airfoil, Node, Ligament, FEA (Finite Element Analysis)

ABSTRACT
This paper investigates the Design and Analysis of the innovative morphing Airfoil using the Auxetic Structure (Chiral Structure). This Structure is selected because it undergo larger displacement with limited Straining of its components and its unique deformation characteristics, which produce theoretical, in-plane Poisson's ratio of -1. Different configuration of chiral structure is compared. Aluminum Alloy AL6061-T651 material is considered for all the structural elements.

The objective of this paper is to investigate the compliance characteristics of the Airfoil with chiral structure as core. Finite Element Model is developed and the structural Analysis is performed. The advantage associated with the use of Auxetic Structure in the Airfoil is investigated by comparing the result from the previous investigations. The results are captured and plotted.

INTRODUCTION
Cellular solids are used widely in a variety of engineering applications. In particular, honeycomb cell structures are very prevalent. The continuing desire for stronger, lighter weight, structural materials for use in aerospace and aircraft applications has made these industries the traditional leaders in the development of honeycomb structures for technological use. However, improved manufacturing processes have made these unique composite materials more affordable and viable for other industries [1].
Compared to the fundamental studies on cellular solids, their practical applications have been limited to the development of stiff and ultra-light sandwich cores for aircraft and aerospace structures, which are related to the honeycombs' out of plane properties[8]. In the drive to develop new and advanced materials for structural applications, factors to consider include how to achieve reduced weight and improved drape ability or conformability (doubly-curved surfaces). The ability to imbue the material, or the system within which the material is incorporated, with smart or intelligent functionality for adaptive control or structural health monitoring capabilities, for example, is also desirable. The lightweight requirement often points to the use of a honeycomb material incorporated within a composite sandwich panel construction. Double curvature, required in nose cones or other body parts for automotive and aerospace vehicles for example, can be achieved with minimum material wastage and damage during production by designing the honeycomb to possess auxetic (negative Poisson's ratio) response [2]. The inventors are challenged with developing specialized materials that mimic elastomeric properties yet are composed of low dampening materials, thereby reducing energy loss under shear for use in the shear layer of a shear band of a tire. A solution may be found in a design of honeycombs. Our previous study on a design of shear flexure with honeycombs shows that cellular solids having negative Poisson's ratio, called auxetic, have high shear flexibility [10]. By changing the honeycomb ligament angle we can achieve negative poissons ratio. We call it as re-entrant hexagonal honeycomb. The re-entrant hexagonal honeycomb is auxetic when deformation is predominantly via flexing or hinging of the cell walls (ligaments). When the ligament length is varied from its original size, its Poisson's ratio will varies accordingly.
The negative Poisson's ratio occurs over a range of strain [8, 9, and 10] and that range is larger in the polymer than in the metal foams. In the above structures and materials, the negative Poisson's ratio arises from the unfolding of the re-entrant cells, and isotropy can be achieved along with the negative Poisson's ratio [5].The allowable range of Poisson's ratio in three dimensional isotropic solids is from -1 to one half . Most common materials have a Poisson's ratio close to one third, however rubbery materials have values approaching one half; they readily undergo shear deformations, governed by the shear modulus G but resist volumetric (bulk) deformation governed by the bulk modulus K, so G << K.].In honeycombs, the negative Poissons ratio behavior implies a stiffening geometric effect, which leads to increase in-plane indentation resistance, shear modulus and compressive strength. An analytical analysis of deformation of these honeycombs allows prediction of the mechanical properties [4]. The honeycomb structure is composed of circular elements or nodes of equal radius r

ISSN 2349-6193
Impact Factor (PIF): 2.243

IJESMR
International Journal OF Engineering Sciences & Management Research

joined by straight ligaments or ribs of equal length L. The ligaments are constrained to be tangential to the nodes. The angle between adjacent ligaments is equal to sixty degrees. Structures exhibiting hexagonal symmetry are mechanically isotropic in-plane. Experiments discussed later confirm isotropy in Poisson's ratio [5]. AN AIRCRAFT structure is defined as morphing when it can change its shape and size during flight. Usually, the term morphing refers to seamless shape changes that are continuous and not to classical discrete aircraft wing adaptation systems, such as flaps or leading and trailing-edge high-lift devices. Such types of morphing can be regarded as directly inspired by the imitation of nature, which has been one of the main guidelines for designers since the beginning of human flight. As the application point of view, chiral honeycomb with circular central node is used in the ribs of wing.

Auxetic Geometry

The Auxetic networks are obtained through the assembly of elliptical elements (nodes), connected by ribs (ligaments) tangent to the nodes as shown in Fig 1 & 2. The parameters defining the auxetic geometry are R, L, t and d.

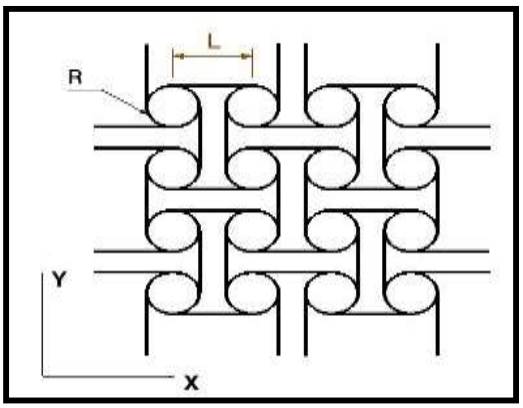

Fig 1: Auxetic Topology Elliptical node

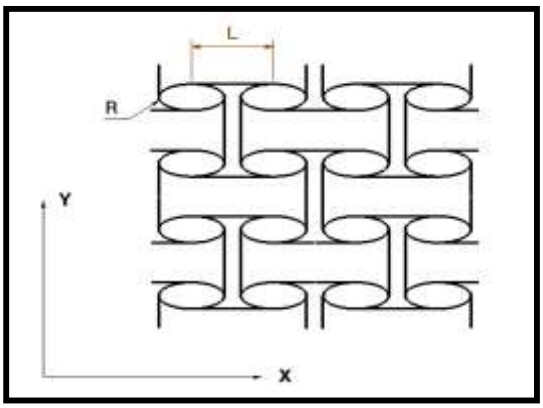

Fig 2: Auxetic Topology Circular node

Where,
R Semi major Span,
R/2 Semi minor Span,
L Ligament length,
T Wall thickness,
d Depth

FE Model of single unit cell

The Auxetic structure was modeled and simulated using commercial finite element modeling software (MSC Nastran and Patran). The mesh size was determined in order to guarantee elements possess all mesh quality parameters (aspect ratio and size at least one 20th of the radius of the cylinder) see Fig 3.

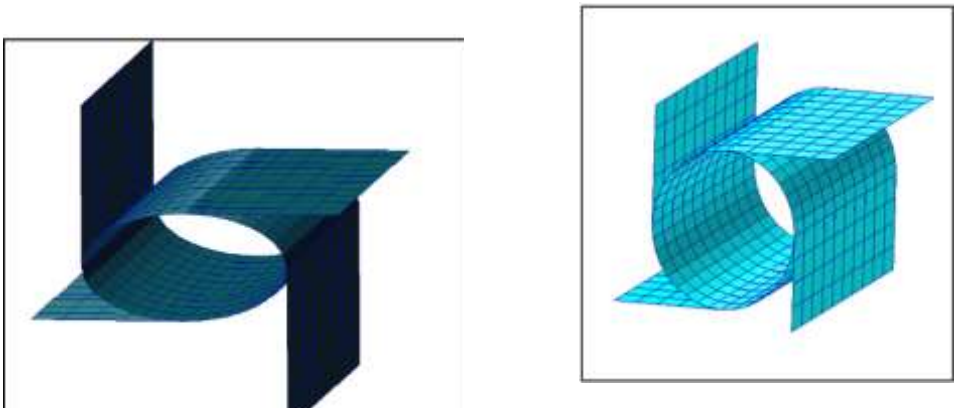

Fig 3: FE Model of the unit cell (Elliptical node & Circular node) with shell elements

ISSN 2349-6193
Impact Factor (PIF): 2.243

IJESMR
International Journal OF Engineering Sciences & Management Research

Deformation Mechanism

The Auxetic structure deform by the action of node rotation and ligament bending Fig.4 shows the node and ligament structure of the auxetic honeycomb predicted from the FE model before and after deformations. The applied tensile load generates a torque on the nodes so that it undergone in-plane rotation.
This rotation induces the momentum on the ligaments connected to the each node and causes them to bend.

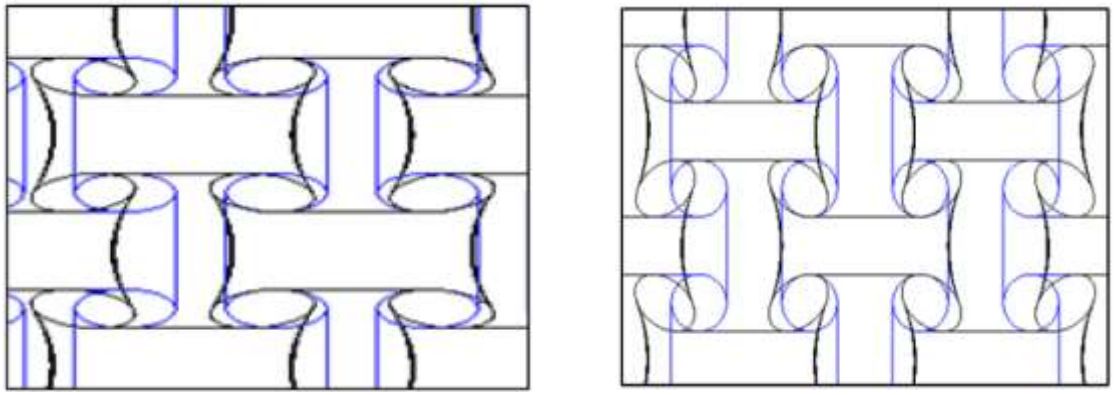

Fig 4: Deformation of an Auxetic Structure Elliptical node and Circular node

Material Selection

The 6000 series Aluminum are alloyed with magnesium and silicon, are easy to machine, and can be precipitation hardened. It has good machinability and possesses good resistance.
It is used in construction of aircraft structures, such as wings and fuselages, more commonly in homebuilt aircraft than commercial or military aircraft. Composition of AL6061-T651 (Table 1).

T651

- Solution heat treated and artificially aged.
- No further straightening after stretching

AIRFOIL CONFIGURATIONS

The NACA airfoils are airfoil shapes for aircraft wings developed by the National Advisory Committee for Aeronautics (NACA). The shape of the NACA airfoils is described using a series of digits following the word "NACA". The parameters in the numerical code can be entered into equations to precisely generate the cross-section of the airfoil and calculate its properties.
Initial investigations on the application of the auxetic geometry to morphing can be found in [35], where the performance of a conformable
Race car wing is analyzed through a numerical model. In [35], the airfoil core is modeled as a homogeneous material with the mechanical properties of a homogenized chiral assembly. This implicitly assumes that the unit cell size is much smaller than the dimensions of the wing.

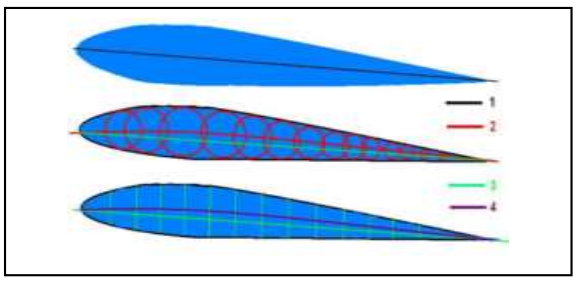

Fig 5: Profile lines – 1: Chord, 2: Camber, 3: Length

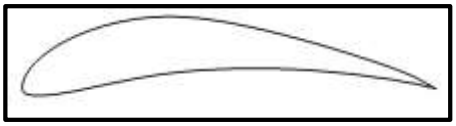

Fig 6: Eppler 420 Airfoil

Subsequent studies [Spadoni and Ruzzene 2006; Spadoni et al. 2006] have instead considered configurations

ISSN 2349-6193
Impact Factor (PIF): 2.243

IJESMR
International Journal OF Engineering Sciences & Management Research

where the cell has dimensions of the order of those of the structure. Both in [35] and in [Spadoni and Ruzzene 2006], an Eppler 420 profile is considered see Fig 6.
Such a highly cambered airfoil is chosen to demonstrate the compliance of the assembly, as the deformations that are sought involve decambering effects See Fig 5. In [Spadoni and Ruzzene 2006] the compliance of the core airfoil, in terms of de-cambering deformations due to aerodynamic loads, was investigated through weakly coupled CFD and linear, electrostatic FE models.
The results showed the strong influence of the core configuration, and specifically how number of cells and L/R ratio can be selected to achieve desired levels of de-cambering deformations for assigned flow conditions.
The main objective of the current paper is to investigate the properties of the auxetic core airfoil. While in [Spadoni and Ruzzene 2006], the loads applied to the FE models were distributed pressures of aerodynamic nature.

Eppler 420Airfoil Properties

- (e420-il) EPPLER 420 AIRFOIL
- Eppler E420 high lift airfoil
- Max thickness 14.3% at 22.8% chord.
- Max camber 10.6% at 40.5% chord
- Source UIUC Airfoil Coordinates Database

DESIGN OF AUXETIC CORE IN AIRFOIL

Chiral structure with elliptically structured central node configuration is placed inside the Eppler 420 airfoil. Reason for keeping these two structures is because of its elastic properties and the coefficient lift properties. Chiral structures have more elastic properties so if small amount of load is enough to bend the structure so it helps to increase the lift properties of the airfoil. 2-D structure of the Airfoil is represented in Figure 7.

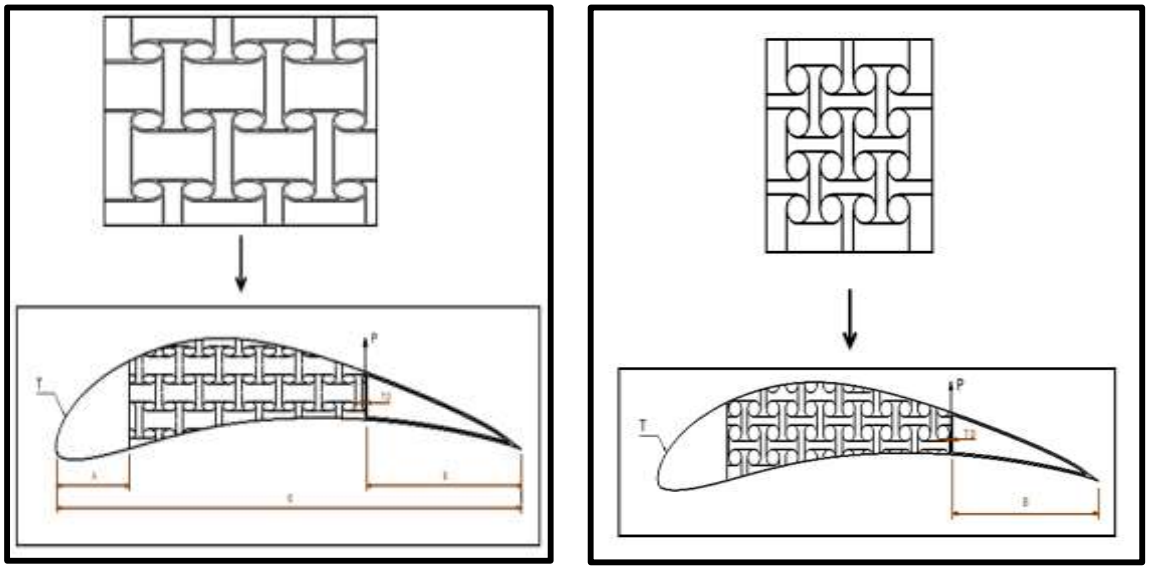

Fig 7: Mapped Auxetic-core configuration Elliptical node and Circular node

Where,

T Skin thickness,
P Applied Load,
TD Trailing edge boundaries,
C Chord

The properties of the structure changes depend on the elemental properties of the elements which are connected between. Each nodes and ligaments inside the airfoil structures boost the airfoil properties so it will leads to high lift coefficient to the drag.

ISSN 2349-6193
Impact Factor (PIF): 2.243

IJESMR
International Journal OF Engineering Sciences & Management Research

The orientation of the elliptical structure changes the properties of the structures. If more load carrying support is on the top surface, orient the elliptical structure to its major length axis. It will carry more load than the minor axis, the advantages over chiral honeycomb with circular node to the chiral honeycomb with elliptical structures is load carrying capacity.

Stress Analysis of Morphing Airfoil with Auxetic Structure

A structural Finite Element model is developed to investigate the ability of the airfoil to undergo large chord-wise deformations while within the linear range of the material. The model is designed using the commercially available software CATIA V5. Then the model is meshed using HYPERMESH. Structural Analysis is done by MSC NASTRAN and PATRAN.

In order to allow de-cambering deformations, the upper and lower portions of the airfoil profile are modeled as a soft material with stiffness 100 times lower than that of the core.

The developed model predicts the de-cambering characteristics of the airfoil corresponding to an imposed concentrated load at the trailing edge as shown in Fig. 8 & 9. The details of the stress analysis are presented in the following sections

Geometrical specifications

The Fig. 8 & 9 shows the geometrical details of the airfoil. The configuration of the core is defined by selecting a periodic, two-dimensional auxetic with specified number of cells and L/R ratio. The resulting geometry is then mapped into the airfoil profile (Eppler 420) through a simple coordinate transformation.

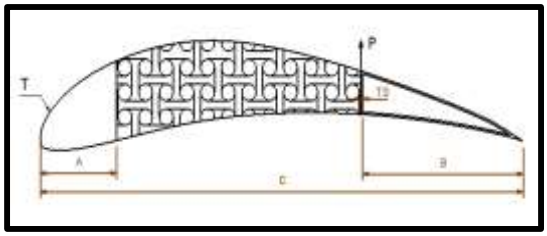

Fig 8: Airfoil and core dimensions Circular Node

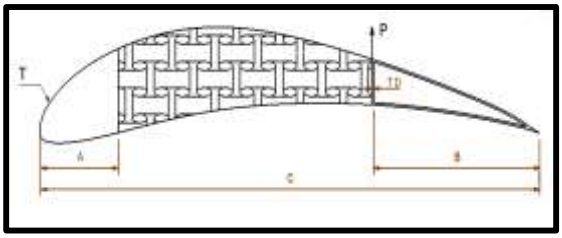

Fig 9: Airfoil and core dimensions elliptical Node

Where,
Chord, C = 700 mm
Length, A = 110 mm
Length, B = 235 mm
Skin thickness, T = 1 mm

The out-of-plane thickness of the structure is 19 mm. The trailing-edge profile TD is 2.54 mm. The ability to carry shear loads illustrated in [Spadoni and Ruzzene 2006] and the potential torsional rigidity of the design due to its negative Poisson's ratio suggest that the classic closed section with stressed skin may not be necessary.

In fact the core itself may provide sufficient torsional and shear-loads carrying capacity, that the skins would only be used to provide the surface continuity dictated by aerodynamic requirements. Additional developments of the concept would therefore require the investigation of the application of flexible skins, able to conform to the airfoil, to allow de-cambering deflections, while maintaining smoothness of the airfoil surface.

Meshing

The process of discretization of the structure is called meshing. The segment of the airfoil is meshed using CQUAD4, CBEAM elements as shown in Fig 10 & 11. Meshing is a laborious work. The quality of meshing is important to get the accurate stress response. All the quality for elements is met during the meshing process. The fine meshing is done at the critical location.

To get the mesh transition from fine mesh to coarse-mesh, tria elements are being used in the model. The tria elements are used away from the region under consideration, which is the fine meshed region.

The following grid points and elements used for meshing of an airfoil are shown below:

Elliptical Node

Number of grid points = 55945
Number of CQUAD4 elements = 4991
Number of CBEAM elements = 150

ISSN 2349-6193
Impact Factor (PIF): 2.243

IJESMR
International Journal OF Engineering Sciences & Management Research

Circular Node
Number of grid points = 54167
Number of CQUAD4 elements = 17206
Number of CBEAM elements = 108

Finite Element Model

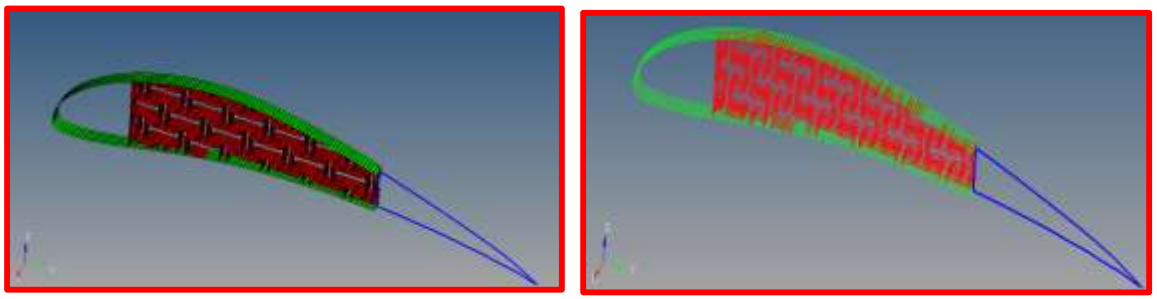

Fig 10: Airfoil and core dimensions elliptical Node

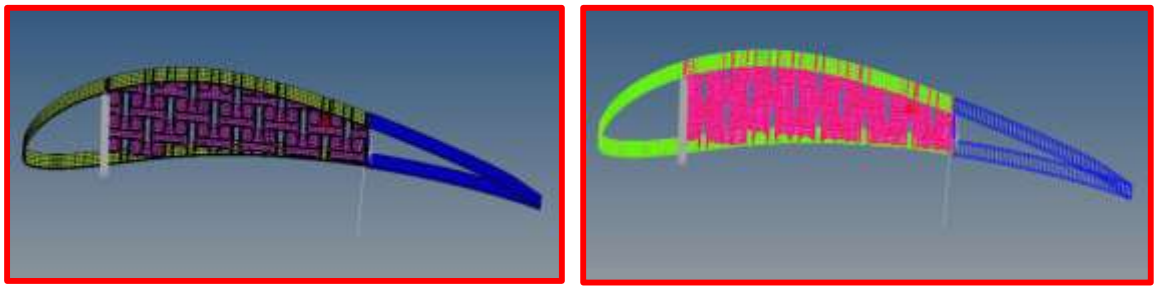

Fig 11: Airfoil and core dimensions Circular Node

Loads and Boundary conditions

CQUAD4 element applied to the skin and the auxetic core. CBEAM element applied to the trailing edge. In the model, the leading edge region is considered completely clamped.
The axial load P is applied to the near the core. The type of analysis is Linear.

Material properties

The material considered for the structure is,
Aluminum Alloy – 6061-T651, with the following properties.
Young's modulus, E = 69 Gpa
Poison's ratio, $\mu = 0.33$
Yield strength, $\sigma y = 276$ MPa
Tangent Modulus Et= 100 MPa
Density, $\rho = 2700$ Kg/m3

RESULTS AND DISCUSSION

The deflections of the wing profile are induced by a concentrated mechanical load applied at the location is shown. The highest stresses appear within the core, and in particular, where ligaments join nodes. As per the result which I have obtained, clearly shows that the airfoil structures which carrying chiral honeycomb with circularly structured central node deflect more with less load than the chiral honeycomb with elliptically structured central node. The orientation of the Elliptically structured node should be reversed.
The displacement and Von-Mises stress for the applied load are tabulated and suitable plots are made for Elliptical node and Circular node.

ISSN 2349-6193
Impact Factor (PIF): 2.243

IJESMR
International Journal OF Engineering Sciences & Management Research

Load VS Trailing Edge Displacement VS Stress Table
Elliptical Node

Load (N)	Displacement (mm)	Stress (Mpa)
5	0.772	19.8
10	1.54	39.6
20	3.09	79.2
30	4.63	119
40	6.17	158
50	7.72	198
60	9.26	238
70	10.8	277
80	12.3	317
90	13.9	357
100	15.4	396
120	18.5	475
140	21.6	555
150	23.2	594

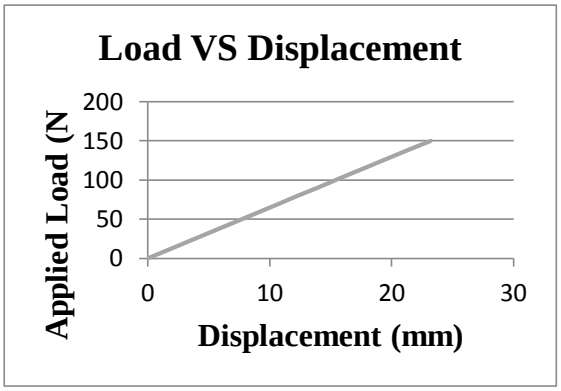

Fig.12 Load VS Trailing Edge Displacement Plot

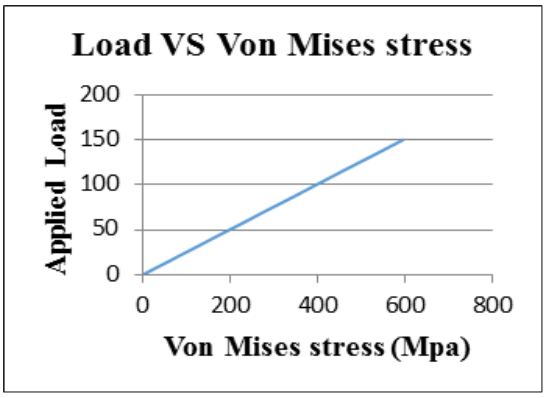

Fig. 13 Load VS von Mises Stress Plot

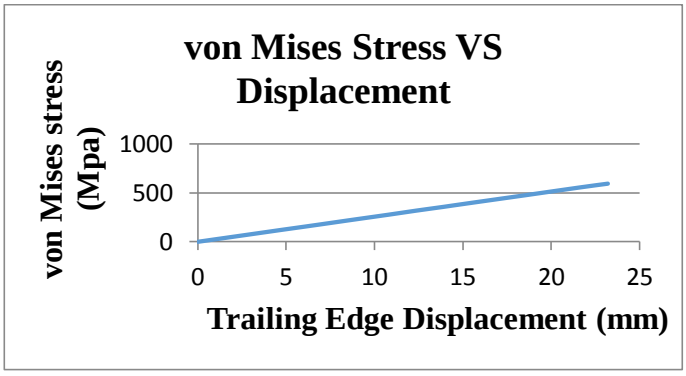

Fig. 14 von Mises Stress VS Trailing Edge Displacement Plot

ISSN 2349-6193
Impact Factor (PIF): 2.243

IJESMR
International Journal OF Engineering Sciences & Management Research

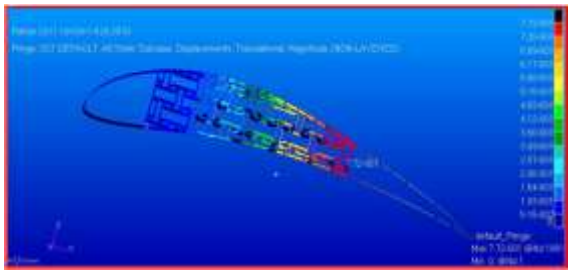

Fig. 15 Trailing Edge Displacement at a Load of 5N

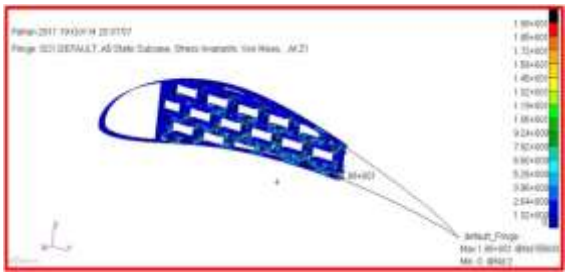

Fig. 16 von-Mises Stress at a Load of 5N

Fig. 17 Trailing Edge Displacement at a Load of 20N

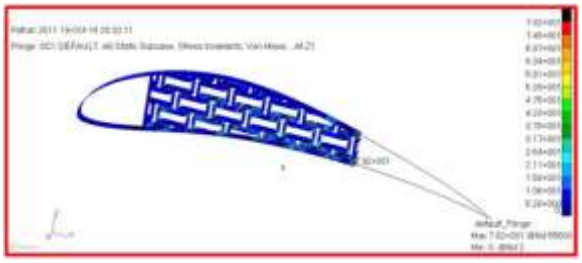

Fig. 18 von-Mises Stress at a Load of 20N

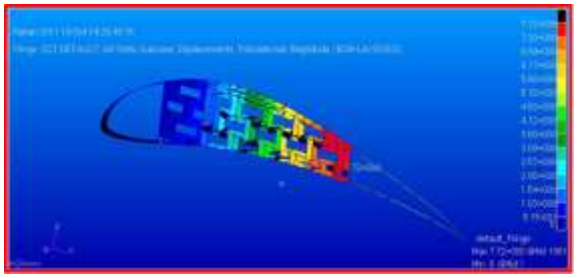

Fig. 19 Trailing Edge Displacement at a Load of 50N

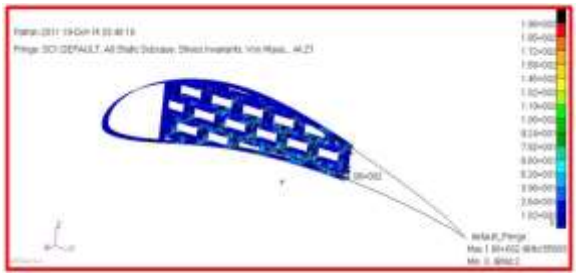

Fig. 20 von-Mises Stress at a Load of 50N

Fig. 21 Trailing Edge Displacement at a Load of 100N

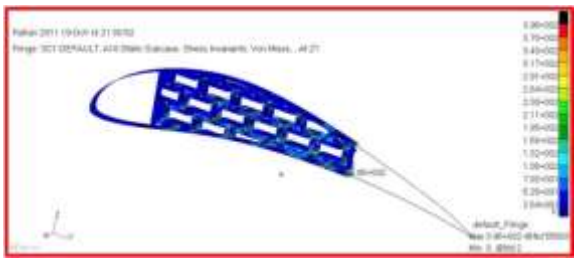

Fig. 22 von-Mises Stress at a Load of 100N

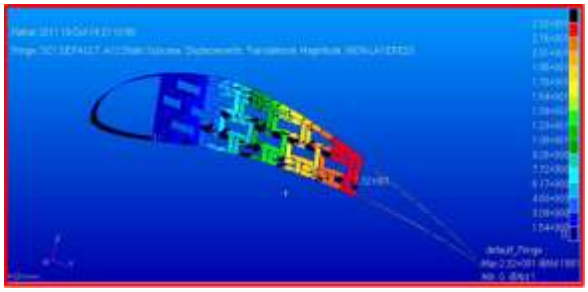

Fig. 23 Trailing Edge Displacement at a Load of 150N

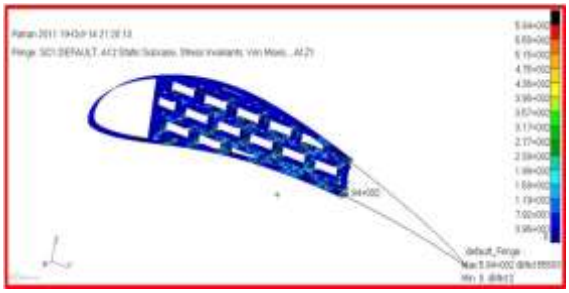

Fig. 24 von-Mises Stress at a Load of 150N

ISSN 2349-6193
Impact Factor (PIF): 2.243

IJESMR
International Journal OF Engineering Sciences & Management Research

10.2.2Circular Node

Load (N)	Displacement (mm)	stress (Mpa)
5	1.12	37.7
10	2.24	75.5
20	4.48	151
30	6.72	226
40	8.95	302
50	11.2	377
60	13.4	453
70	15.7	528
80	17.9	604
90	20.1	679
100	22.4	755
120	26.9	906
140	31.3	1060
150	33.6	1130

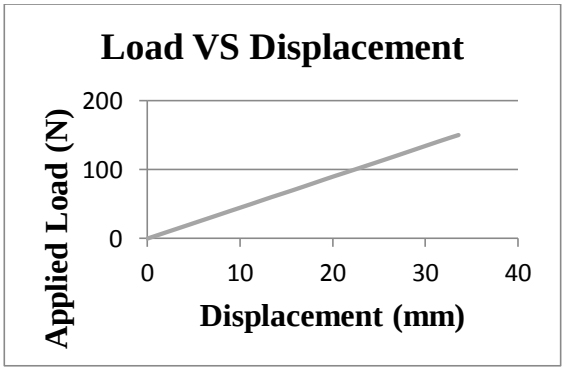

Fig.25 Load VS Trailing Edge Displacement Plot

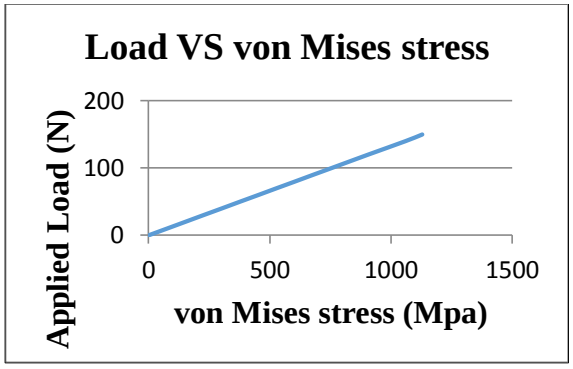

Fig. 26 Load VS von Mises Stress Plot

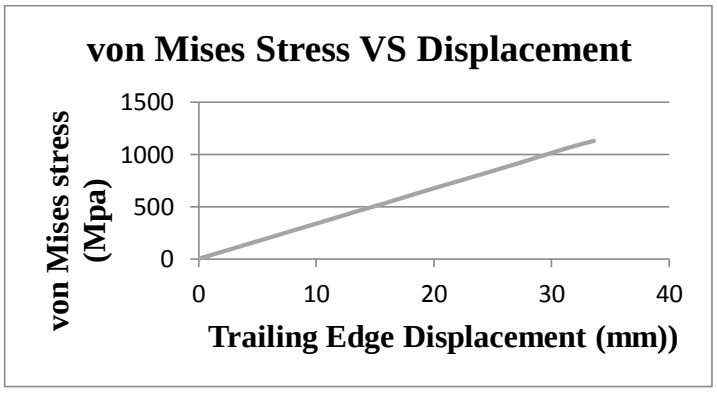

Fig. 27 von Mises Stress VS Trailing Edge Displacement Plot

ISSN 2349-6193
Impact Factor (PIF): 2.243

IJESMR
International Journal OF Engineering Sciences & Management Research

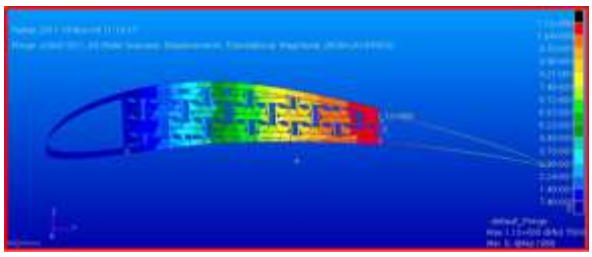

Fig. 28 Trailing Edge Displacement at a Load of 5N

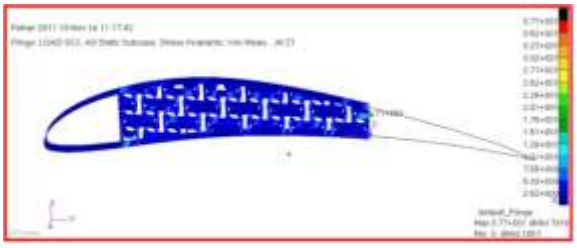

Fig. 29 von-Mises Stress at a Load of 5N

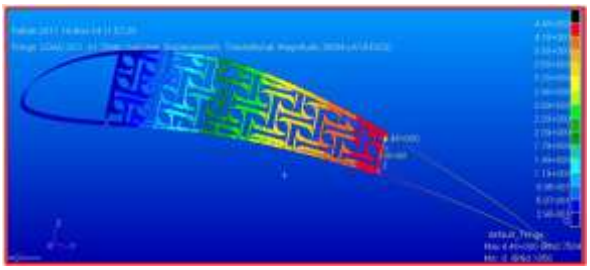

Fig. 30 Trailing Edge Displacement at a Load of 20N

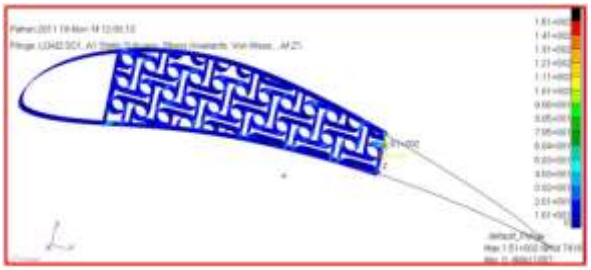

Fig. 31 von-Mises Stress at a Load of 20N

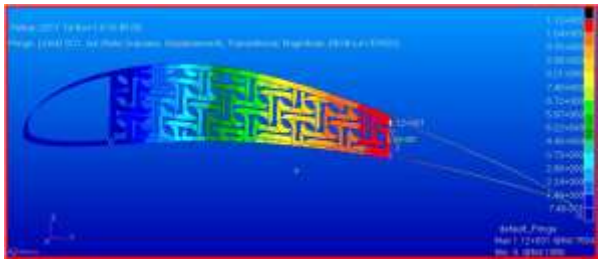

Fig. 32 Trailing Edge Displacement at a Load of 50N

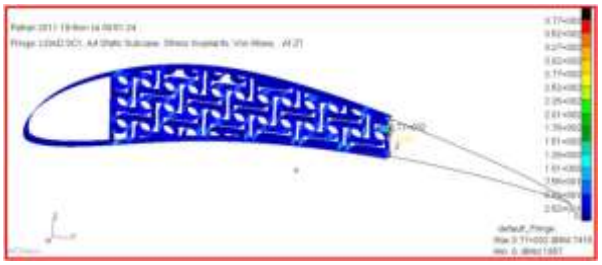

Fig. 33 von-Mises Stress at a Load of 50N

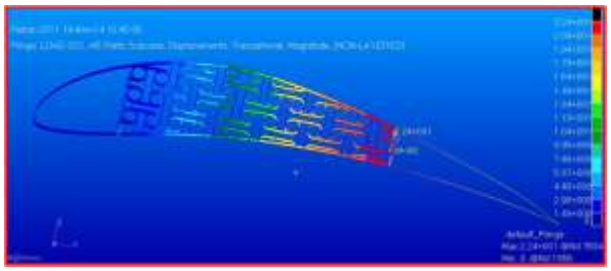

Fig. 34 Trailing Edge Displacement at a Load of 100N

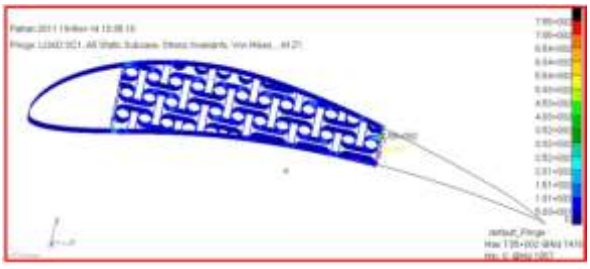

Fig. 35 von-Mises Stress at a Load of 100N

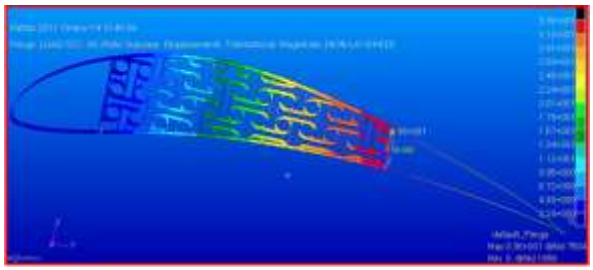

Fig. 36 Trailing Edge Displacement at a Load of 150N

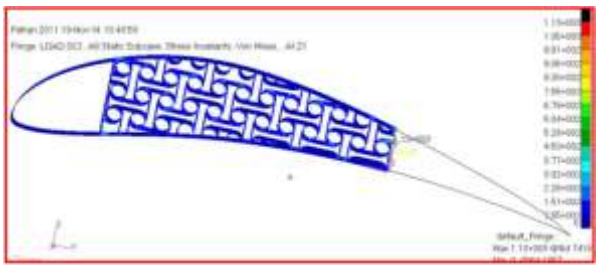

Fig. 37 von-Mises Stress at a Load of 150N

TABLES

ISSN 2349-6193
Impact Factor (PIF): 2.243

IJESMR
International Journal OF Engineering Sciences & Management Research

Table 1: Composition of AL6061-T651

Materials	Composition
Silicon Si	0.40% – 0.8%
Ferrous Fe	0.70%
Copper Cu	0.15% – 0.40%
Manganese Mn	0.15%
Magnesium Mg	0.8% – 1.2%
Chromium Cr	0.04% – 0.35%
Zinc Zn	0.25%
Titanium Ti	0.15%
Balance, Aluminum Al	

CONCLUSION AND FUTURE WORK

- This Paper investigates the properties of Auxetic Structure for both Circular and Elliptical node.
- The considered configuration finds potential application as part of a morphing airfoil.
- The proposed design, an Auxetic structure is accommodated within the airfoil profile to provide it with chord wise bending compliance, combined with the ability of carrying torsional loads.
- The compliance characteristics of airfoils with Circular node and Elliptical node designs are investigated with the objective of assessing the ability of the structure to undergo large deflections while remaining in the linear range of the material, and the strong influence of the core design on the overall performance of the airfoil.
- In this paper we have compared the negative Poisson's effect of both Circular node and Elliptical node, each node is connected with four ligaments tangentially.
- The structure deform by the action of node rotation and ligament bending.
- The negative Poisson's effect increases with increase in thickness of the system and decrease of ligament length.
- Dynamic characterization of the proposed truss core airfoil should also be performed.
- The same analyses suggest the opportunity of achieving significant performance variations through the proper selection of a limited number of parameters which define the core geometry.
- A natural application for this concept is aeroelastic tailoring.
- Future investigations will therefore address the performance of three dimensional wings with chiral ribs, or of wings with an internal, three dimensional network which extends the configuration herein investigated.

REFERENCES

[1] Properties of a chiral honeycomb with a Poisson's ratio -1 Int. J. of Mechanical Sciences, 39, 305-314, (1996). Diagrams at bottom
[2] Evans KE. Chem. Ind. 1990, 654-657
[3] Stretch, but without the wrinkles by Marianne Freiberger.
[4] Alessandro Spadoni and Massimo Ruzzene, Mechanical and thermal properties of chiral honeycombs, http://coloradolinux.com/~sjg/USNCTAM06/search/M3/Abstract_259.pdf
[5] Properties of a chiral honeycomb with a Poisson's ratio -1 D. Prall, R. S. Lakes Int. J. of Mechanical Sciences, 39, 305-314, (1996).
[6] R. S. Lakes, Foam structures with a negative Poisson's ratio, Science , 235 1038-1040 (1987).

IJESMR
International Journal OF Engineering Sciences & Management Research

[7] Finite element analysis of effective mechanical properties, vibration and acoustic performance of auxetic chiral core sandwich structureshrishikesh joshi, clemson university
[8] Gellatry, R. A., Bijlaard, P. P., and Gallaherm, R. H., (1965), "Thermal Stress and Instability of Sandwich Cylinders on Rigid Supports," Journal of Aircraft, vol. 2, no. 1, pp. 44-8,
[9] Chiral honeycomb meso-structures for shear flexure
US 20110240194 A1
[10] Sigmund, O., (2008), "Systematic Design of Metamaterials by Topology Optimization," in IUTAM Symposium on Modeling Nanomaterials and Nanosystems, Aalborg, Denmark. pp. 151-9.
[11] C. Thill, J. Etches, I. Bond, K. Potter and P. Weaver Advanced Composites Centre for Innovation and Science (ACCIS) Department of Aerospace Engineering, University of Bristol, UK
[12] It was shown by NASA researchers that a hyper-elliptically swept planform wing with a cambered span, with a separate hyper-elliptical span wise profile, has aerodynamic advantage over flat wings. Such a wing, referred to as Hyper-Elliptical Cambered Span (HECS), Ibrahim Elgayar
[13] Wilson S. A new face of aerospace honeycomb. Mater Des 1990;11(6):323–6.
[14] Bitzer T. Honeycomb marine applications. J ReinfPlast Compos 1994;13(4):355–60.
[15] Thompson RW, Matthews FL. Load attachments for honeycomb panels in racing cars. Mater Des 1995;16(3):131–50.
[16] Price T, Timbrook RL. Structural honeycomb panel building system, Patent number US6, 253, 530 B1. July 3, 2001.
[5] Lu TJ. Heat transfer efficiency of metal honeycombs.Int J Heat Mass Transfer 1999;42(11):2031–40.
[17] Gu S, Lu TJ, Evans AG. On the design of two-dimensional cellular metals for combined heat dissipation and structural load capacity. Int J Heat Mass Transfer 2001;44(11):2163–75.
[18] Hyun S, Torquato S. Optimal and manufacturable two-dimensional, Kagomelike cellular solids. J Mater Res 2002;17(1):137–44.
[19] Wen T, Tian J, Lu TJ, Queheillalt DT, Wadley HNG. Forced convection in metallic honeycomb structures. Int J Heat Mass Transfer 2006;49:3313–24.
[20] Wang Bo, Wang Bin, Cheng G. Multifunctional design of sandwich panels with Kagome-like cores.ActaMateriae Compos Sinica 2007;24(3):109–15.
[21] Lakes R. Materials with structural hierarchy. Nature 1993;361:511–5.
[11] Pugno N. Mimicking nacre with super-nanotubes for producing optimized super-composites. Nanotechnology 2006;17(21):5480–4.
[22] Gao H. Application of fracture mechanics concepts to hierarchical biomechanics of bone and bone-like materials. Int J Fract 2006;138:101–37.
[23] Pugno N, Carpinteri A. Design of micro-nanoscale bio-inspired hierarchical materials. Philos Mag Lett 2008;88(6):397–405.
[24] Carpinteri A, Pugno N. Mechanics of hierarchical materials. Int J Fract 2008;150:221–6.
[25] Zhao Q, Kreplak L, Buehler MJ. Hierarchical structure controls nanomechanical properties of vimentin intermediate filaments. PLoS ONE 2009;4(10):e7294.
[26] Fratzl P, Weinkamer R. Nature's hierarchical materials. Progr Mater Sci 2007;52:1263–334.
[27] Chen Q, Pugno N. Modeling the elastic anisotropy of woven hierarchical tissues. Compos Part B: Eng 2011; 42(7):2030–7.
[18] Chen Q, Pugno N. Mechanics of hierarchical 3-D nanofoams. EurophysLett 2012;97:26002.
[28] Burgueno R, Quagliata MJ, Mohanty AK, Mehtad G, Drzale LT, Misraf M. Hierarchical cellular designs for load-bearing biocomposite beams and plates. Mater SciEng A 2005;390:178–87.
[29] Fan H, Jin F, Fang D. Mechanical properties of hierarchical cellular materials. Part I: Analysis. Compos SciTechnol 2008; 68:3380–7.
[30] K. E. Evans, M. A. Nkansah, I. J. Hutchinson, S. C. Rogers, Molecular network design, Nature 353 (1991) 124
[31] F. Scarpa, J. R. Yates, L. G. Ciffo, S. Patsias, Dynamic crushing of auxetic open-cell polyurethane foam, Proceedings of the Institution of Mechanical Engineers Part C-Journal of Mechanical Engineering Science 216 (12) (2002) 1153–1156
[32] Smart shape memory alloy chiral honeycomb M.R. Hassana, F. Scarpab, M. Ruzzenec, N.A. Mohammedd
[33]Auxetic materials for sports applications Mohammad Sanamia , Naveen Raviralaa , Kim Aldersona , Andrew Aldersonb
[34] http://emps.exeter.ac.uk/engineering/research/materials-manufacturing/interests/multi-func/auxetic/

ISSN 2349-6193
Impact Factor (PIF): 2.243

IJESMR
International Journal OF Engineering Sciences & Management Research

[35] Bornengo et al. 2005] D. Bornengo, F. Scarpa, and C. Remillat, "Evaluation of hexagonal chiral structure for morphing airfoil concept", Proc. Inst. Mech. Eng. G, J. Aerosp. Eng. 219:3 (2005), 185–192.
[36] [Büter et al. 2001] A. Büter, U. C. Ehlert, D. Sachau, and E. Breitbach, "Adaptive rotor blade concepts: direct twist and camber variation", pp. 1–12 (Section 19) in Active control technology for enhanced performance operational capabilities of military aircraft, land vehicles and sea vehicles (Braunschweig, 2000), RTO Meeting Proceedings 51, NATO Research and Technology Organization, Neuilly-sur-Seine, 2001, Available at ftp://ftp.rta.nato.int//PubFullText/RTO/MP/RTO-MP-051/MP-051-MSSM-19.PDF. Report RTO-MP-051.
[37] [Cadogan et al. 2004] D. Cadogan, T. Smith, F. Uhelsky, and M. MacCusick, "Morphing airfoil wing development for compact package unmanned aerial vehicles", pp. 3205–3217 in 45th AIAA/ASME/ASCE/AHS/ASC Structures, Structural Dynamics and Materials Conference (Palm Springs, CA, 2004), AIAA, Reston, VA, 2004, Available at http://www.aiaa.org/content.cfm?pageid=2. Paper #2004-1807. Prall D, Lakes RS.Properties of a chiral honeycomb with a Poisson's ratio of -1.Int J MechSci 1997;39(3):305–14.
[38] A. Alderson, K. L. Alderson, D. Attard, K. E. Evans, R. Gatt, J. N. Grima, W. Miller, N. Ravirala, C.W. Smith, K. Zied, "Elastic constants of 3-, 4- and 6- connected chiral and anti-chiral honeycombs subject to uniaxial inplane loading", Composite Science and Technology, Vol. 70, 2010, pp. 1042-1048.
[39] Rodriguez AR. Morphing aircraft technology survey. In: Proceedings of 45th AIAA aerospace sciences meeting and exhibit. Reno, NV, January, 2007 [AIAA Paper 2007-1258].
[40] A. Baron, B. Benedict, N. Branchaw, B. Ostry, J. Pearsall, G. Perlman, J. Selstrom, Morphing Wing (MoW), Department of Aerospace Engineering, Rept. ASEN 4018, University of Colorado at Boulder, Dec. 2003.
[41] L.F. Campanile, Lightweight shape-adaptable airfoils: A new challenge for an old dream, in: I.B. David Wagg, Paul Weaver, MichealFriswellChichester (Eds.), Adaptive Structures: Engineering Application, John Wiley and Sons Ltd., West Sussex, UK, 2007, pp. 89–136.
[42] T.L. Pinkerton, R.W. Moses, A Feasibility Study to Control Airfoil Shape Using THUNDER, 1997.
[43] H. Namgoong, W.A. Crossley, A.S. Lyrinthzis, Aerodynamic optimization of a morphing airfoil using energy as an objective, AIAA Journal 45 (9) (2007) 2113–2124.
[44] M. R. Hassan, F. Scarpa, M. Ruzzene, N. A. Mohammed, "Smart shape memory alloy chiral honeycomb", Materials Science & Engineering A, Vol. 481-482, pp. 654-657.